

Room Temperature Lasing of InAs/GaAs Quantum Dots in the Whispering Gallery Modes of a Silica Microsphere

Sébastien Steiner, Jean Hare* and Valérie Lefevre-Seguin

Laboratoire Kastler Brossel – École normale supérieure

24, rue Lhomond – F-75231 Paris cedex 05 – France †

(Dated: July 21, 2005)

We have achieved low threshold lasing of self-assembled InAs/GaAs quantum dots (QD) coupled to the evanescent wave of the high- Q whispering gallery modes (WGM) of a silica microsphere. In spite of Q -spoiling of WGM due to diffusion and refraction on the high index semiconductor sample, room temperature lasing is obtained with fewer than 10^3 QD. This result implies an efficient deconfinement of the WGM field toward the semiconductor, which is interpreted as a mode reconstruction process.

PACS numbers: 42.50.-p, 42.55.-f, 78.67.-n

Semiconductor nanostructures providing efficient confinement of charge carriers have attracted considerable interest for several decades. Advances in semiconductor technology have allowed for the fabrication of heterostructures where bandgap discontinuities provide a binding potential in one or several dimensions. The resulting density of states is “engineered” to provide a stronger coupling to the electromagnetic field, favorable for ever more efficient light sources. In quantum dots (QDs) especially, the 3D confinement leads to the formation of “atom like” discrete levels, thus concentrating oscillator strength on discrete transitions, favoring efficient atom–light interaction. Though significant departures from a truly atom-like system have been characterized, the large oscillator strength associated with the fundamental (recombination) transition makes QDs very promising elementary emitters for both classical and quantum light emitting devices. This transition is characterized by an optical dipole moment in excess of 10 a.u. (1 a.u. = $e a_0$), significantly greater than for atoms or ions, and by a moderate homogeneous broadening (down to below 1 GHz) [1], at least at cryogenic temperatures.

QDs are therefore perfectly suited for solid-state Cavity quantum electrodynamics (CQED) experiments, aimed at controlling spontaneous and stimulated emission properties of electron-hole pairs. CQED relies on electromagnetic-mode density engineering, quite similar to that performed on electronic densities of states [2, 3]. The most natural way of performing this kind of experiment consists in embedding the QDs in a semiconductor microcavity, obtained by lithography and subsequent etching, which can be a micropillar, a microdisk, or a photonic bandgap cavity. The two figures of merit for a microcavity are its mode volume in cubic wavelengths V/λ^3 , and its quality factor Q : the high interest of semiconductor microcavities resides in the very small mode volumes which can be achieved, although they suffer from moderate quality factors [4, 5, 6].

An interesting alternative is the use of fused silica microspheres sustaining small volume whispering-gallery modes (WGM) with ultrahigh quality factors resulting

from high transparency and very small residual roughness. The WGM are formed by successive total internal reflection along the sphere equator, leading, for a typical sphere of $100\ \mu\text{m}$ in diameter, to mode volumes in the range of $1000\ \mu\text{m}^3$ and to a quality factor Q as high as 10^{10} [7, 8]. Beside TE or TM polarization, these modes are described by 3 integer numbers n, ℓ, m characterizing the electric field distribution $E \propto f_{n\ell}(r) Y_\ell^m(\theta, \varphi)$. While n is the number of antinodes of the radial function $f_{n\ell}(r)$, ℓ and m are the usual angular “quantum” numbers, associated to $\ell - |m| + 1$ anti-nodes in the polar direction. The modes with $n = 1$ and $|m| = \ell$ are confined at the wavelength scale around the sphere equator, with an evanescent wave roughly decaying as $\exp(-\kappa r)$ in the surrounding air, with $\kappa \approx 2\pi/\lambda$. They verify $2\pi a \approx \ell \lambda/N$ where a and N are the sphere radius and refractive index respectively. Coupling of silica microspheres with embedded rare-earth ions has been thoroughly investigated in the last decade [9, 10, 11, 12, 13], and strong coupling CQED with evanescently coupled laser cooled atoms is also a very promising field [14, 15, 16, 17].

In this letter, we report the laser operation of an original combination of a silica microsphere and InAs/GaAs self-organized QDs used as the amplifier medium. We had to overcome two challenging problems: the poor radiative efficiency of the QDs *at room temperature* resulting from thermal promotion of carriers to the continuum states of the wetting layer, and the strong broadening of WGMs induced by the high refractive index sample. Despite these difficulties, we nevertheless achieved a cw laser effect with thresholds as low as $200\ \mu\text{W}$ in absorbed pump power.

We used a sample supplied by J.-M. Gérard (sample C9B34). It was grown by molecular beam epitaxy (MBE), starting from a (1,0,0) GaAs substrate. The epitaxial structure consisted in: 30 nm GaAs buffer layer, 30 nm $\text{Al}_{0.15}\text{Ga}_{0.85}\text{As}$, 50 nm GaAs, a layer of InAs QDs, 20 nm GaAs, 10 nm $\text{Al}_{0.15}\text{Ga}_{0.85}\text{As}$, and on top a 2.1 nm GaAs cap layer. The $\text{Al}_{0.15}\text{Ga}_{0.85}\text{As}$ quantum well provides a barrier to prevent non-radiative carrier recombination at the surface. The capping layer on the QDs

was kept as thin as possible in order to maximize the evanescent coupling to the WGM.

The InAs layer was deposited so as to obtain a thickness gradient on the wafer, and our sample was chosen in the wafer area of large QDs. This choice enhances the binding energy of carriers and therefore maximizes their average population and the overall radiative efficiency at room temperature. The sample was furthermore etched to produce an array of square $4 \times 4 \mu\text{m}$ micromesas about 200 nm in height, 40 μm apart from one another. The QD density being about $5 \cdot 10^9 \text{ cm}^{-2}$, each mesa contains approximately 800 QDs.

Their photoluminescence (PL), excited by a focused diode laser at $\lambda_{\text{pump}} = 778 \text{ nm}$ (1.59 eV) with a flux of typically 10^3 W/cm^2 , is centered at $\lambda_{\text{PL}} = 1075 \text{ nm}$ (1.15 eV). Its observed linewidth of 100 nm (110 meV) is mainly due to inhomogeneous broadening resulting from size dispersion, while homogenous broadening due to phonon scattering is about 2.5 THz (10 meV) at room temperature [18]. The wetting layer's PL is observed at 872 nm (1.420 eV), with a much smaller linewidth (about 15 nm).

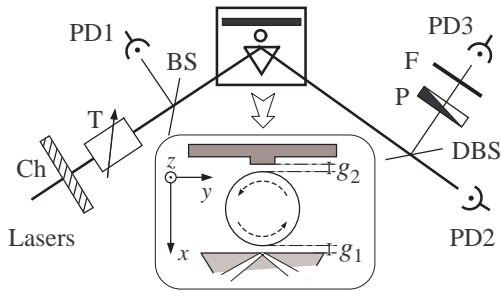


FIG. 1: Scheme of experimental setup. Ch : chopper; T : attenuator; BS : beam-splitter; DBS : dichroic beam-splitter; P : polarization analyzer; F : Wratten 87C filter. Bottom inset: WGM coupling geometry

The experimental setup is sketched in Fig. 1. Its main features have been described in previous work (see e.g. Ref. [9]). The main advantage of prism-coupling over alternative techniques is the ability to optimize input coupling of the pump while keeping good output coupling of the PL.

In order to benefit from resonant pumping of the QDs at $\lambda_{\text{pump}} \simeq 780 \text{ nm}$ the sphere is placed between the prism and the GaAs sample. This configuration has two key advantages: (i) only the QDs actually coupled to a WGM can be excited, and (ii) the PL extracted through the prism is necessarily emitted inside the WGMs.

However, this configuration makes the precise alignment of the setup more difficult, the microsphere being almost stuck between two millimeter-sized objects, which must be carefully positioned parallel to one another, and also to the sphere stem, in order to prevent any unwanted contact. One also has to control independently the two

coupling gaps: g_1 between prism and sphere, and g_2 between the sphere and the sample (top of mesa), as shown in the inset of Fig. 1.

As mentioned above, bringing the high index GaAs sample into the WGM evanescent wave is expected to greatly reduce the latter's quality factor by providing efficient tunnelling of light outside the cavity. We indeed observe significant sample-induced broadening of the WGM resonances, but no more than the usual broadening due to the prism. This is well understood via a simple model describing the modification of the WGM evanescent field by a plane dielectric. It can be shown that this modification is characterized by the Fresnel reflection coefficient for the evanescent wave:

$$r \approx \frac{i\sqrt{N_{\text{eff}}^2 - 1} - \sqrt{N_D^2 - N_{\text{eff}}^2}}{i\sqrt{N_{\text{eff}}^2 - 1} + \sqrt{N_D^2 - N_{\text{eff}}^2}}, \quad (1)$$

where N_{eff} is the WGM effective index (close to N in the case of grazing incidence), and N_D the index of the dielectric. This reflection coefficient accounts for a frequency shift proportional to the real part of r , and a line broadening proportional to the imaginary part of r . With $N_{\text{eff}} \approx N \approx 1.45$ and $N_D \approx 1.76$ for SF11 or 3.3 for GaAs (at 1060 nm), one gets $r \simeq 0.05 + i 0.999$ for the prism, and $r \approx -0.77 + i 0.63$ for GaAs. This means that, while the index of SF11 gives an almost vanishing shift and a large broadening, the high index of GaAs mainly results in a large shift and a rather moderate broadening [20]. These predictions were experimentally confirmed by using a flat (un-etched) pure GaAs sample.

Positioning a given mesa in the field of a strongly confined WGM is absolutely critical. A rough alignment of the setup is first achieved using a stereomicroscope, as shown in the inset of Fig. 2. It is then necessary to PZT-control the positioning of the selected mesa. This is optimized by monitoring the influence of the mesa directly on the WGM spectral properties, due to the effect described above. As an example, Fig. 2 shows the records obtained when scanning the position of the mesa in a direction y approximately parallel to the equator, with the gaps (x) and the height (z) kept constants (see Fig. 1 for definition of axes). The exponential behavior of the evanescent wave results in a Gaussian dependance $\exp(-\kappa y^2/a)$ of intensity versus y . Because the height of the mesa is larger than κ^{-1} , the mesa can be seen, in a first approximation, as a small area sample. The behavior of the width or the shift of the line thus appears as a convolution of the square mesa profile and the gaussian, with an expected full width at half maximum of about 5 μm , in good agreement with the experimental results[21]. Due to a slight tilt (about 0.5°) between the sphere axis and the vertical axis z , the best coupled mode was a mode with $m = \ell - 7$. The records obtained for this mode when z is scanned (not shown here) actually reveal two antinodes of the polar intensity distribution. In these scans, the observed shift/broadening ratio (28%)

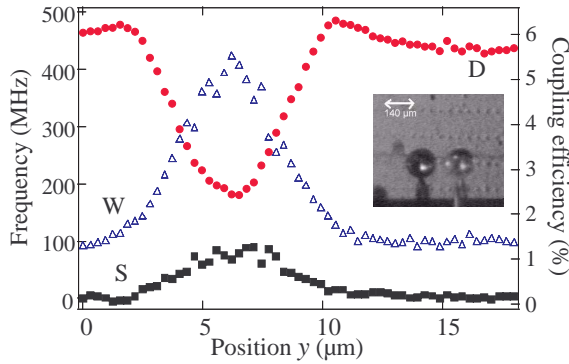


FIG. 2: Evolution of the width (Δ), shift (\blacksquare) and coupling (\bullet) when the sample is scanned along y . *Inset:* Photograph of the sphere in front of the GaAs sample. The sphere is on the right and the image to the left is its reflection. The small dots are the $4 \mu\text{m} \times 4 \mu\text{m}$ mesa, revealed by grazing illumination.

is much smaller than the expected value of 78%, and this reveals an extra loss mechanism, attributed to the strong light scattering at the edges of the mesa. The settings described above were achieved with two DBR laser diodes operating at $\lambda_1 = 772 \text{ nm}$ and $\lambda_2 = 1060 \text{ nm}$ in order to characterize the prism–sphere and sphere–sample coupling parameters at both the pumping and the emission wavelengths.

For the laser experiment, the pump laser was a widely tunable Littman-Metcalf extended cavity laser diode (Newport/EOEI 2010) with a central wavelength of about 780 nm. It was tuned to a strongly confined mode providing a resonant enhancement of the pumping field. The observed shift/broadening ratio indicates that about one third of the pump power contributes to photoexcitation of the sample (above the bandgap of GaAs). Special care had to be taken to filter out a small luminescence from this laser-diode in the 900–1100 nm range. This parasitic signal which otherwise would hide the QD’s emission was eliminated thanks to a dispersion prism inserted at the exit of the pump laser. The QD emission, outcoupled from the WGMs via the prism, was finally monitored using an InGaAs photodiode (Hamamatsu G3476-10) providing sensitivity at the pW level (PD3 in Fig. 1). To extract the PL signal from the noise, the pump beam was chopped at a frequency of about 200 Hz, and a lock-in amplifier was used. We also inserted in front of PD3 three sheets of gelatine IR filter (Kodak Wratten 87C) to further eliminate the residual pump light.

Because the QD active medium–field coupling and the resonance broadening exhibit the same exponential behaviour, there is no preferred g_2 value for laser operation. However, a simple model taking into account the losses due to the prism shows that the lowest threshold should be obtained when $g_2 = 0$. We therefore worked with the sample in contact with the sphere, a situation which furthermore provides much better mechanical sta-

bility. The gap g_1 was set close to critical coupling for the loaded cavity. In this situation, it was possible to observe the onset of lasing, hallmark by a well pronounced threshold in the pump/emission characteristic curve of the microsphere cavity.

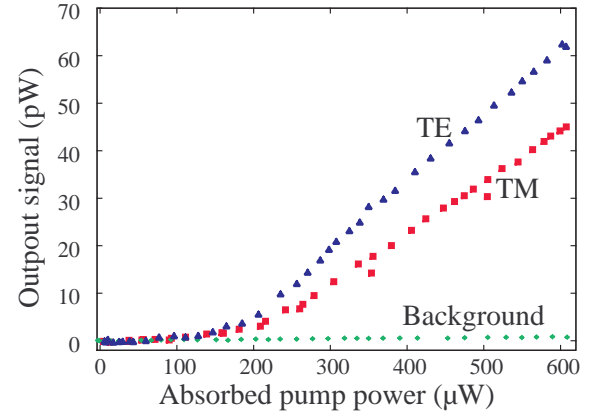


FIG. 3: Emission vs. absorption laser characteristics. The background curve shows the residual fraction of pump laser PL at wavelength higher than 900 nm.

Figure 3 shows such a laser characteristic curve for both TE and TM polarization, with the threshold of $200 \mu\text{W}$, the lowest observed. In this figure, the “output signal” is the raw detected signal, not corrected for collection and detection efficiency. The “absorbed pump power” is the power lost from the incident beam into the sphere (including scattering) as monitored by photodiodes PD1/PD2 in Fig. 1.

These curves were obtained for a $140 \mu\text{m}$ sphere, pumped into a $n = 1$, $m = \ell - 6$, TE polarized WGM. Due to the small extracted power, and the lack of a low noise, cooled spectroscopic camera, it was not possible to record a spectrum of this laser. However the observed attenuation when inserting an additional sheet of Wratten filter or a RG1000 filter confirmed that the wavelength of the emitted light was 1000 nm or higher. As the coupling of the mesa to the sphere has been optimized for a WGM with $n = 1$ and $m = \ell - 6$, we can confidently assume that the lasing WGMs are also modes with $n = 1$ and $\ell - m \approx 6$. The ℓ value is not limited by the same overlap constraints, and can *a priori* cover the gain spectral range leading to ℓ values lying between 550 and 600. The mode volume is about $5000 \mu\text{m}^3$ (for $\lambda \sim 1075 \mu\text{m}$). The measured width of these WGMs at 1080 nm was $\Gamma/2\pi = 1 \text{ GHz}$.

We now estimate the number N_{th} of excited QDs at threshold, as a function of the absorbed pump power P_{th} . This can be written as:

$$N_{\text{th}} = (\eta_{\text{pump}} P_{\text{th}} / \hbar \omega_{\text{pump}}) \times \alpha_{\text{capt}} \eta_{\text{rad}} \tau \quad (2)$$

where η_{pump} is the *effective* fraction of the pump power, α_{capt} the capture efficiency of the QDs, η_{rad} their ra-

diative efficiency and τ their radiative lifetime. The radiative lifetime and efficiency are known to be ≈ 800 ps and $\approx 10\%$ (at room temperature) respectively, and the capture efficiency α_{capt} (for the carriers photoexcited in the AlGaAs well) is assumed to be close to one. The effective pump power is first limited by the factor 30% deduced from the shift/broadening ratio. An additional factor of 7% comes from the width of the useful zone inside the AlGaAs quantum well: this is only 70 nm while the absorbtion length of the pump is $\alpha^{-1} \approx 1 \mu\text{m}$. This finally leads to $\eta_{\text{pump}} \approx 2\%$. With the experimental value $P_{\text{th}} = 200 \mu\text{W}$, one gets $N_{\text{th}} \approx 600$, which is satisfactorily consistent with the total number of QDs in the mesa.

The number N_{th} can be related to the WGM electric field E_{QD} experienced by the QDs by using a simple model of the laser, based on semiclassical rate equations[22]. In this model the cavity emission rate reads $W = \Omega_R^2/\gamma_{\text{hom}}$ where $\Omega_R/2\pi$ is the Rabi frequency, and $\gamma_{\text{hom}}/2\pi$ is the homogenous linewidth. Using the above mentioned values for the relevant parameters, one gets a *maximal* Rabi frequency $\Omega_R/2\pi = 2 \text{ GHz}$ and a *maximal* cavity emission rate $W/2\pi \approx 1.6 \text{ MHz}$. Thus the number of excited dots involved in the lasing process is :

$$N_{\text{th}} = \Gamma/W \simeq 600 \times (E_{\text{max.}}/E_{\text{QD}})^2. \quad (3)$$

From the asymptotic law $E(a)/E_{\text{max}} \simeq 2.28 \ell^{-1/3}$ linking the surface field to the maximal fields in the WGMs of an isolated sphere [19], one expects $E_{\text{QD}}/E_{\text{max}} \lesssim 0.26$. Expression (3) clearly shows that this last relation does not fit properly with the experimentally measured threshold and is not compatible with the average number of QDs in a mesa. It rather suggests that the structure of the WGM field is significantly modified by the presence of the mesa. In other words, the field is partially deconfined from the sphere to the high index sample. We believe that this mechanism explains our observations when studying different mesas: although they show the same PL characteristics, some lase while others do not, everything else being equal. Indeed the mode reconstruction, which depends on the precise size and structure of the mesa, is expected to vary from one mesa to the other. It would be very interesting to further explore this effect experimentally.

The results presented here clearly demonstrate the potential of dielectric microcavities coupled to semiconductor nanostructures, a combination which is expected to gain further applications in the near future.

The authors acknowledge Jean-Michel Gérard for providing the InAs/GaAs sample and for his interest in these experiments. They warmly thank Jean-Michel Raimond and Serge Haroche for fruitful and encouraging discussions. This work was partly supported by CNRS-Japan Science and Technology contract (Stanford/Ens ICORP “Quantum Entanglement” Project) and by European Community (QUBITS Network).

* Corresponding author: jean.hare@lkb.ens.fr

† Laboratoire Kastler Brossel is a laboratory of École normale supérieure and Université P. & M. Curie, associated to C.N.R.S. (UMR 8552).

- [1] P. Borri, W. Langbein, S. Schneider, U. Woggon, R. L. Sellin, D. Ouyang, and D. Bimberg, *Phys. Rev. Lett.* **87**, 157401 (2001).
- [2] S. Haroche, in *Fundamental Systems in Quantum Optics*, edited by J. Dalibard, J.-M. Raimond, and J. Zinn-Justin (North Holland, Amsterdam, 1992), p. 767.
- [3] J. Rarity and C. Weisbuch, eds., *Microcavities and Photonic Bandgaps*, Series E: Applied Sciences – volume 324 (Kluwer Academic Publishers, Dordrecht, 1996).
- [4] P. Michler, A. Kiraz, C. Becher, W. Schoenfeld, P. Petroff, L. Zhang, E. Hu, and A. Imamoglu, *Science* **290**, 2282 (2000).
- [5] E. Moreau, I. Robert, J. M. Gérard, I. Abram, L. Manin, and V. Thierry-Mieg, *Appl. Phys. Lett.* **79**, 2865 (2001).
- [6] C. Santori, D. Fattal, J. Vučković, G. S. Solomon, and Y. Yamamoto, *Nature* **419**, 594 (2002).
- [7] V. B. Braginsky, M. L. Gorodetsky, and V. S. Ilchenko, *Phys. Lett. A* **137**, 393 (1989).
- [8] L. Collot, V. Lefèvre-Seguin, M. Brune, J. M. Raimond, and S. Haroche, *Europhys. Lett.* **23**, 327 (1993).
- [9] V. Sandoghdar, F. Treussart, J. Hare, V. Lefèvre-Seguin, J.-M. Raimond, and S. Haroche, *Phys. Rev. A* **54**, R1777 (1996).
- [10] W. von Klitzing, E. Jahier, R. Long, F. Lissillour, V. Lefèvre-Seguin, J. Hare, J.-M. Raimond, and S. Haroche, *Electr. Lett.* **35**, 1745 (1999).
- [11] F. Lissillour, P. Feron, N. Dubreuil, P. Dupriez, M. Poulain, and G. M. Stephan, *Electr. Lett.* **36**, 1382 (2000).
- [12] M. Cai, O. Painter, K. J. Vahala, and P. C. Sercel, *Opt. Lett.* **25**, 1430 (2000).
- [13] I. Protsenko, P. Domokos, V. Lefèvre-Seguin, J. Hare, J.-M. Raimond, and L. Davidovich, *Phys. Rev. A* **59**, 1667 (1999).
- [14] F. Treussart, J. Hare, L. Collot, V. Lefèvre, D. S. Weiss, V. Sandoghdar, J.-M. Raimond, and S. Haroche, *Opt. Lett.* **19**, 1651 (1994).
- [15] H. Mabuchi and H. J. Kimble, *Opt. Lett.* **19**, 749 (1994).
- [16] D. W. Vernooy, A. Furusawa, N. P. Georgiades, V. S. Ilchenko, and H. J. Kimble, *Phys. Rev. A* **57**, R2293 (1998).
- [17] R. Long, T. Steinmetz, P. Hommelhoff, W. Hänsel, T. W. Hänsch, and J. Reichel, *Phil. Trans. Roy. Soc. London* **361**, 1375 (2003).
- [18] P. Borri, W. Langbein, J. Mørk, J. M. Hvam, F. Heinrichsdorff, M.-H. Mao, and D. Bimberg, *Phys. Rev. B* **60**, 7784 (1999).
- [19] F.-M. Treussart, Ph.D. thesis, Université Paris VI (1997).
- [20] Even at 778 nm the large imaginary part of $N_D \approx 3.67 + i 0.29$ gives $r \approx -0.78 + i 0.54$, leading to the same conclusion.
- [21] The small increase of the coupling efficiency on each side of the central drop indicates the crossing of critical coupling for prim–sphere interaction, initially over-coupled.
- [22] It is legitimate to consider the QD and cavity at resonance because the homogenous linewidth is much greater than the FSR of the cavity ($\approx 1.6 \text{ nm}$).